

Document downloaded from:

<http://hdl.handle.net/10251/100046>

This paper must be cited as:

Moreno Marro, O.; Cárdenas Estela, J.; Atarés Huerta, LM.; Chiralt A. (2017). Influence of starch oxidation on the functionality of starch-gelatin based active films. *Carbohydrate Polymers*. 178:147-158. doi:10.1016/j.carbpol.2017.08.128



The final publication is available at

<https://doi.org/10.1016/j.carbpol.2017.08.128>

Copyright Elsevier

Additional Information

27 1. Introduction

28 Nowadays, most of the food packaging systems are based on petroleum-derived
29 synthetic plastics, whose production has increased exponentially over the past two
30 decades (Tharanathan, 2003). Nevertheless, the utilization of these materials involves a
31 serious environmental problem and high recycling costs (Moreno et al., 2014). In order
32 to deal with this issue, current research focuses on the development of biodegradable
33 polymers from renewable sources (Byun and Kim, 2014; Cazón, 2016).

34 Of the natural polymers available, starch is one of the most promising
35 polysaccharides, since it is an abundant, low cost edible material (Barnett, 2011; Cazón,
36 2016, Moreno et al., 2015) and capable of being processed by the usual treatments
37 applied in synthetic materials (Moreno et al., 2016). Native starch becomes thermoplastic
38 (TPS) when thermally treated with plasticizers, which reduces the melting temperature
39 below that of decomposition, thus allowing it to be moulded into a determined shape
40 (Jiménez et al., 2012). However, TPS films also show some drawbacks when compared
41 to oil-derived synthetic polymers, such as its highly hydrophilic nature, giving rise to water
42 sensitivity and a poor water vapour barrier capacity. Starch retrogradation is also an
43 inconvenience due to the fact that its mechanical properties worsen throughout storage
44 (Ortega-Toro et al., 2014).

45 Properties of TPS films have been improved by blending with other biopolymers. More
46 specifically, blends with gelatin have been previously reported to yield films with
47 improved resistance and elongation capacity (Acosta et al., 2015; Fakhoury et al., 2012).
48 Moreno et al. (2016) obtained starch-gelatin based films by thermo-processing and found
49 no improvement in the water sensitivity, which suggests the need for developing new
50 strategies to produce more hydrophobic starch matrices, or crosslinking processes
51 which enhance the functionality of the starch material. In this sense, the oxidation of
52 starch, giving rise to dialdehyde formation (DAS), can be used to promote the
53 crosslinking capacity of the chains, while increasing the hydrophobicity of the matrix.
54 During the oxidizing process, an oxidative cleavage of C-2 and C-3 bond of the
55 anhydroglucose units of the native starch is produced (Yu et al., 2010, Du et al., 2008),
56 yielding a reduction in hydroxyl groups to form carboxyl and carbonyl groups. The
57 condensation reaction between carbonyl and amino groups also enables DAS to act as
58 crosslinking agent with proteins (Rhim et al., 1998; Wang et al., 2015). In this context, it
59 may be hypothesized that starch oxidation may be an adequate strategy to improve
60 functional properties of biodegradable films based on starch and gelatin, on the basis of
61 the crosslinking of polymers, thus reinforcing the inner matrix, and improving the

62 mechanical behaviour and water resistance of the films. In fact, Rhim et al. (1998)
63 observed improved rigidity, resistance to fracture and extensibility, as well as reduced
64 water solubility, when DAS was added to soy protein films (5:100 mass ratio). On the
65 other hand, the reaction between carbonyls of reducing sugars and protein amino groups
66 led to the formation of Maillard compounds, thus resulting in film browning. The increase
67 in the number of carbonyl groups reduced the thermal stability of DAS (Soliman et al.,
68 1997; Zhang et al., 2007), which can compromise the thermoprocessing of DAS-gelatin
69 blends. Heating DAS-gelatin blends could, hence, extend the reaction between both
70 polymers, resulting in an unsuitable material.

71 On the other hand, the inner reinforcement of the matrix induced by the crosslinking
72 effect could enhance the retention of bioactive compounds, leading to a more controlled
73 release when applied to foodstuffs. The incorporation of ethyl lauroyl arginate (N- α -
74 lauroyl-L-arginine ethyl ester monohydrochloride, LAE) into DAS-gelatin films, can
75 provide them with antimicrobial properties, while introducing more amino and carbonyl
76 groups in the system, which could also participate in the crosslinking process, affecting
77 the physical properties of the films. LAE is a potent food antimicrobial agent, derived
78 from lauric acid, L-arginine, and ethanol with a wide spectrum of antimicrobial activity,
79 even at low concentrations (Muriel-Galet et al., 2015). LAE has been reported to cause
80 cell growth inhibition or death by increasing the permeability of the cell membrane, as a
81 consequence of the membrane protein denaturation (Rodriguez et al., 2004). Thus, LAE
82 is a promising antimicrobial additive considered as GRAS (Generally recognized as safe)
83 by the FDA, and accepted as food additive E243 in Europe (Hawkins et al., 2009;
84 Higuera et al., 2013). Its antimicrobial properties have been widely studied in different
85 food systems, either directly incorporated into the food formulations or as component of
86 packaging materials. LAE has been effective at controlling the growth of different bacteria
87 in food products such as roasted turkey (Jiang et al., 2011), cold-smoked salmon (Kang
88 et al., 2014), frankfurters (Martín et al., 2010), cheese (Soni et al., 2012) or chicken
89 breast (Nair et al., 2014). Its antimicrobial effectiveness has also been proved when
90 incorporated into different packaging films of polymers, such as chitosan (Higuera et al.,
91 2013; Ma et al., 2016), zein (Kashiri et al., 2016), EVOH (Muriel-Galet et al., 2015)
92 or pullulan (Pattanayaiying et al., 2015).

93 The present study aims to evaluate the effect of different degrees of starch oxidation
94 and LAE incorporation on the functional properties of starch-gelatin blend films, obtained
95 by casting method. The crosslinking effect in oxidized starch-gelatin matrices was
96 assessed in comparison with non-oxidized starch. Moreover, the tensile and optical

97 properties and barrier capacity to water vapour after 5 weeks of storage were analysed
98 in order to evaluate the development of the crosslinking effect throughout time.

99 **2. Material and Methods**

100

101 **2.1. Materials**

102 The following materials were employed to obtain the films: Corn starch (CS) (Roquette
103 Laisa España, S.A., Valencia, Spain); Bovine gelatin type A (BG) (Sancho de Borja, S.L.,
104 Zaragoza, Spain); Sodium periodate (SP) (Fluka Analytical, Sigma–Aldrich Chemie
105 GmbH, Steinheim, Germany); Ethyl lauroyl arginate (LAE) at 10% w/v in ethanol
106 (Vedeqsa, Lamirsa, Terrassa, Spain) and glycerol as plasticizer (Panreac Química S.A.,
107 Castellar de Vallès, Barcelona, Spain).

108 Stock cultures, *Escherichia coli* (CECT 101) and *Listeria innocua* (CECT 910),
109 employed for the antimicrobial activity analysis, were supplied by the Spanish Type
110 Culture Collection (CECT, Burjassot, Spain). Tryptone Soy Broth, Agar bacteriological
111 and Buffered peptone water were provided by Scharlab, (Barcelona, Spain).

112 The reagents used for film conditioning (magnesium nitrate or phosphorus pentoxide)
113 and overall migration test (ethanol, acetic acid and isooctane) were all supplied by
114 Panreac Química S.A., Castellar de Vallès, Barcelona, Spain.

115

116 **2.2. Oxidation of Starch**

117 The oxidation of CS was carried out by using SP as oxidizing reagent following a
118 modification of the method described by Yu et al. (2010). CS was dispersed and gently
119 stirred (10% w/v) in distilled water, then, SP was added obtaining two different
120 SP:Glucose unit molar ratios (1 or 0.5), to obtain two different oxidation levels in the
121 starch samples. The reaction was kept in the dark for four hours at 35 °C. The solution
122 reached a value of pH 3.5 once the components were mixed. Both oxidized starch (OS)
123 samples were washed with distilled water three times, while being homogenised with a
124 rotor stator homogenizer, Ultraturrax (T25, Janke and Kunkel, Germany) at 8,000 rpm
125 for 30 seconds, and subsequently vacuum filtered (MZ 2C NT, Vacuubrand GMBH + CO
126 KG, Wertheim, Germany). The final solids obtained were used for film preparation, taking
127 into account the water content, which was determined by desiccating both samples in a
128 vacuum oven (60°C-24h), and then stored in desiccators with P₂O₅ until constant weight
129 was reached.

130 To verify the different degree of starch oxidation by using two molar ratio of SP (1 or
131 0.5 SP:Glucose molar ratios), the aldehyde content of each sample was determined, as
132 reported by Yu et al. (2010), through the conversion of aldehydes into oximes at 50°C
133 for 2 h, using hydroxylamine hydrochloride. To this end, the OS samples (0.2 g) were
134 added in hydroxylamine hydrochloride (25 mL of a 0.25 M solution) and pH was adjusted
135 to 5, using the adequate volume of 0.1 M NaOH solution throughout the reaction. This
136 reaction was also carried out with native starch, as a control, determining the required
137 volume of the NaOH solution to maintain pH=5. The aldehyde content was quantified
138 from the NaOH volume difference with respect to the control, as moles of aldehyde per
139 g of OS sample.

140

141 2.3. *Film preparation*

142 Six film formulations were prepared using glycerol as plasticizer: three control blend
143 formulations based on starch or DAS and gelatin (mass ratio 1:1) (named OR_0,
144 OR_0.5, OR_1, according to the molar ratio of oxidant used) and three active
145 formulations based on the same blends with LAE (OR_0LAE, OR_0.5LAE, OR_1LAE).

146 The preparation of the films was carried out using the casting method, by blending
147 two separate dispersions of both starch and gelatin in distilled water (2% wt.). All of the
148 starch dispersions were homogenized in a rotor stator homogenizer, Ultraturrax, for 1
149 minute at 8,000 rpm, to ensure a complete dispersion of the compound. Then, to induce
150 starch gelatinization, starch dispersions were immersed in a thermostatic bath at 100°C,
151 for 30, 45 or 60 min, respectively for native and oxidized starch with 0.5 or 1.0 molar ratio
152 of SP, and cooled down to room temperature. Additionally, BG dispersion was prepared
153 with magnetic stirring (30 min at 40°C). Both starch and BG dispersions were mixed (1:1
154 mass ratio) to obtain the control films (OR_0, OR_0.5, OR_1), with the incorporation of
155 glycerol in a polymer:glycerol mass ratio of 1:0.25. Moreover, in order to obtain the active
156 films (OR_0, OR_0.5LAE, OR_1LAE) LAE was added in a polymer:LAE mass ratio of
157 1:0.1. All of the film-forming formulations were kept under magnetic stirring for 30 min,
158 and then, the right amount was poured into Teflon plates (150 mm diameter) to assess
159 1.5 g of dry solids on each plate, corresponding to 84 g dry solids/dm². After drying for
160 48 h at 45%RH and 25 °C, the films were separated from the plates and stored for one
161 and five weeks at 25°C and 53% RH (in desiccators with saturated solutions of
162 magnesium nitrate) prior to analyses.

163

164 2.4. *Microstructural and physical characterization of films.*

165 2.4.1. Film microstructure.

166 The film samples were conditioned in desiccators containing P₂O₅ for 48 h in order to
167 eliminate the water content; then, the films were immersed in liquid nitrogen to obtain
168 cryfractured cross sections. All of the samples were mounted on copper stubs and, after
169 platinum coating, images of the films' cross section were obtained by Field Emission
170 Scanning Electron Microscopy (FESEM), using a ZEISS®, model ULTRA 55 (Germany)
171 Microscope. An accelerating voltage of 2 kV was used for the observation.

172

173 2.4.2. Tensile properties and thickness

174 The tensile behaviour of the films was determined following the standard method
175 ASTM D882 (2001). Prior to every test, the films were conditioned at 53% RH for one
176 and five weeks to evaluate the crosslinking effect throughout time. A texture analyzer
177 (TA-XTplus, Stable Micro Systems, Surrey, United Kingdom) was employed to obtain the
178 stress–strain curves and the following parameters were determined: Elastic modulus
179 (EM, MPa), tensile strength (TS, MPa) and elongation at break (% E). Firstly, the
180 thickness of all of the film formulations was measured at four different points by using a
181 hand-held digital micrometer (Electronic Digital Micrometer, Comecta S.A., Barcelona,
182 Spain). Then, film stripes (25mm wide, 100 mm long) were mounted in the film extension
183 grips and stretched at 50 mm min⁻¹ until breaking. 12 replicates per formulation were run.

184

185 2.4.3. Water content and barrier properties of the films.

186 The moisture of the film samples, conditioned at 53 % RH, was determined by
187 applying a two-step gravimetric method. Firstly, the samples were desiccated in a
188 vacuum oven (60°C-24h) and, secondly, stored in desiccators with P₂O₅ until constant
189 weight was reached. The final results were expressed as g of water per 100 g of dry film.
190 Six replicates per formulation were considered.

191 The water vapour permeability (WVP) of the films was determined according to Mc
192 Hugh et al. (1993), following a modification of the ASTM E96-95 gravimetric method
193 (1995). Prior to the test, the thickness of all the samples was measured at six points, as
194 described above. Round film samples (35mm diameter) of each formulation were

195 secured on Payne permeability cups (Elcometer SPRL, Hermelle/s Argenteau, Belgium),
196 with the outwards-facing side in contact with the air during drying . Before securing the
197 films, 5 mL distilled water was placed (100 % RH) inside each cup, and then the cups
198 were placed inside desiccators containing an oversaturated magnesium-nitrate solution
199 in order to generate 53 % RH. Each pre-equilibrated cabinet was fitted with a fan to
200 provide a strong driving force across the film for water vapour diffusion. The cabinets
201 were stored at 25 °C, weighing the cups periodically (± 0.00001 , ME36S Sartorius,
202 Germany) every 1.5 h, until steady state had been reached (24 h). Four replicates per
203 formulation were considered.

204 The oxygen permeability (OP) of the films was determined following the standard
205 method ASTM D3985-95 (2005). Measurements were taken using an OX-TRAN (Model
206 2/21 ML Mocon Lippke, Neuwied, Germany), at 53% RH and 25°C and 50 cm² exposed
207 area. The films were exposed to pure nitrogen flow on one side and pure oxygen flow on
208 the other side. The OP was calculated by dividing the oxygen transmission rate by the
209 difference in oxygen partial pressure between the two sides of the film, and multiplying
210 by the average film thickness, which was measured at six points before the test. Two
211 replicates per formulation were made.

212

213 2.4.4. Optical properties.

214 The infinite reflectance spectra (R_{∞}) of the film samples (400 to 700nm) was obtained
215 with a spectrophotometer MINOLTA, model CM-3600d (Minolta CO, Tokyo, Japan),
216 measuring on the side of the films facing the air during drying. To this end, the
217 measurements were taken on both black (R_0) and white (R) backgrounds. Additionally,
218 the spectrum of the white background was measured (R_g). Once all the spectra were
219 obtained, the internal transmittance of the films (T_i), an indicator of the transparency, was
220 calculated, using the Kubelka–Munk theory (Hutchings, 1999) for multiple scattering. The
221 same theory allowed R_{∞} , (reflectance for an infinite film thickness) to be obtained, which
222 was used to calculate the CIE-L*a*b* parameters (CIE, 1986), using illuminant D65 and
223 observer 10°. The colour coordinates L* (lightness), C_{ab}^* (chrome) and h_{ab}^* (hue) were
224 calculated according to Atarés et al. (2010). Six samples per formulation were measured.

225

226 2.4.5. Film solubility and swelling in water.

227 A modification of the method described by Balaguer et al., (2011) was applied to
228 determine the solubility and swelling (water uptake capacity) of the films. Film samples
229 were cut into 3 x 3 cm squares and dried for 2 weeks in desiccators over P₂O₅ in order
230 to reduce the water content to practically zero. Firstly, the initial dry weight (W_d^i) of the
231 samples was taken, and then the dry films were immersed in 10mL of distilled water in
232 glass containers, gently stirred and kept in contact for 24h at 25°C. Directly afterwards,
233 the solvent was poured in a filter, retaining the film sample, the remaining surface water
234 was removed and the final wet weight (W_w^f) was measured. These wet samples were
235 dried till constant weight to evaluate the mass of residual solids in the film after soaking
236 (W_d^f). The solubility of the films was expressed as the weight loss (WL %, g/g dry film)
237 of the samples (Equation 1), while the water uptake capacity (ΔW %, g water/g dry film)
238 was calculated by Equation 2. Four replicates per formulation were considered.

$$239 \quad WL\% = \frac{W_d^i - W_d^f}{W_d^i} \cdot 100 \quad (\text{Equation 1})$$

240

$$241 \quad \Delta W\% = \frac{W_w^f - W_d^f}{W_d^f} \cdot 100 \quad (\text{Equation 2})$$

242

243 2.4.6. Overall migration

244 The overall migration of the films conditioned for 1 week at 53% RH was determined
245 according to the current legislation (Commission Regulation (EU) No 10/2011). Film
246 samples were immersed in 50 mL of simulant, keeping a contact ratio of 6 dm² of
247 sample/kg of simulant. Three food simulants were used: Simulant A (ethanol 10% v/v,
248 simulating hydrophilic foods), simulant B (acetic acid 3% w/v, simulating hydrophilic acid
249 foods) and simulant D2 (isooctane, simulating lipophilic foods, with free fats at the
250 surface). All the samples were kept in contact with the simulants for 10 days at 20°C (test
251 number OM1). Directly after the contact time, the film samples were removed from the
252 simulants, which were evaporated until dry. Finally, the obtained residue was weighed
253 and the results were expressed as milligrams of the total constituents released per dm²
254 of contact surface (mg/dm²). All of the tests were run in duplicate.

255

256 2.5. *Thermogravimetric analysis (TGA)*

257 The films were characterized as to their thermal stability using a thermogravimetric
258 analyzer (TGA/SDTA 851e, Mettler Toledo, Schwerzenbach, Switzerland). Each sample
259 film (about 3 mg) was heated from room temperature to 600 °C, under nitrogen flow (50
260 mL/min), at 10°C/min. Two replicates per formulation were obtained.

261

262

263

264 2.6. *ATR FTIR Spectroscopy analysis*

265 The attenuated total reflectance (ATR) FTIR spectra of the different films were
266 obtained in a Thermo Nicolet 5700 Fourier transform infrared spectrometer (FTIR). The
267 average spectra were collected from 64 accumulations with a resolution of 4 cm⁻¹ in the
268 4000-400 cm⁻¹ range, from five different locations of the same specimen.

269

270 2.7. *In vitro antimicrobial properties of the films.*

271 The antimicrobial activity of the films was analyzed *in vitro* against *Escherichia coli*
272 (CECT 101) and *Listeria innocua* (CECT 910). Both strains were initially frozen in TSB
273 with 30% glycerol, and regenerated by inoculation in 10 mL TSB. After incubation (24 h
274 at 37°C), 10µl were transferred into 10 ml TSB, which was incubated for 24 h at the same
275 temperature to obtain a work culture in exponential phase of growth.

276 Film samples were UV treated prior to the microbial assay. TSB tubes of 10 mL were
277 inoculated with 10⁴ CFU/mL and a film portion of 5.3 cm of diameter was introduced in
278 each tube. Inoculated tubes without film were used as inoculum control. All tubes were
279 incubated for 24 h at 37 °C, then, they were ten-fold diluted in order to obtain bacteria
280 enumeration in TSA medium. All the tests were run in duplicate

281

282 2.8. *Statistical analysis*

283 The statistical analysis of the data was performed through an analysis of variance
284 (ANOVA) using Statgraphics Centurion XVI s for Windows 5.1 (Manugistics Corp.,
285 Rockville, Md.). Fisher's least significant difference (LSD) at the 95 % confidence
286 level was used to compare treatments.

287

288 **3. Results and discussion**

289 *3.1. Microstructure and crosslinking analysis in the films.*

290 The degree of starch oxidation in starch samples treated with 0.5 or 1 SP:Glucose
291 molar ratio was 0.467 and 0.898, expressed as moles/g sample, which prove the different
292 extent of dialdehyde formation, according to the molar ratio of the oxidant. The effect of
293 starch oxidation on the blend film's structure and the crosslinking process has been
294 assessed through the analysis of the film's microstructure, FTIR spectra and thermal
295 behaviour (thermogravimetric analysis: TGA). Pure starch films obtained with different
296 molar ratios of the oxidant (0, 0.5 and 1.0) were included in the FTIR and TGA analysis
297 to better understand interactions in starch-gelatin films.

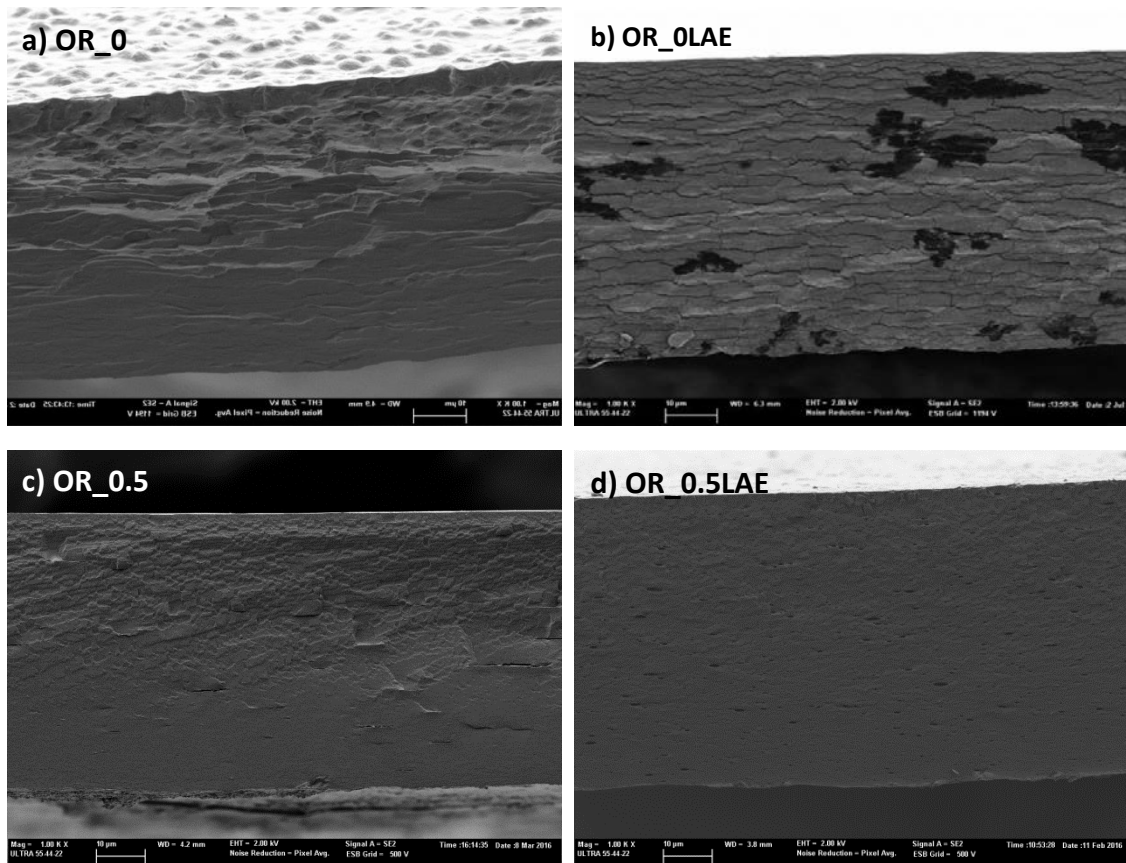
298

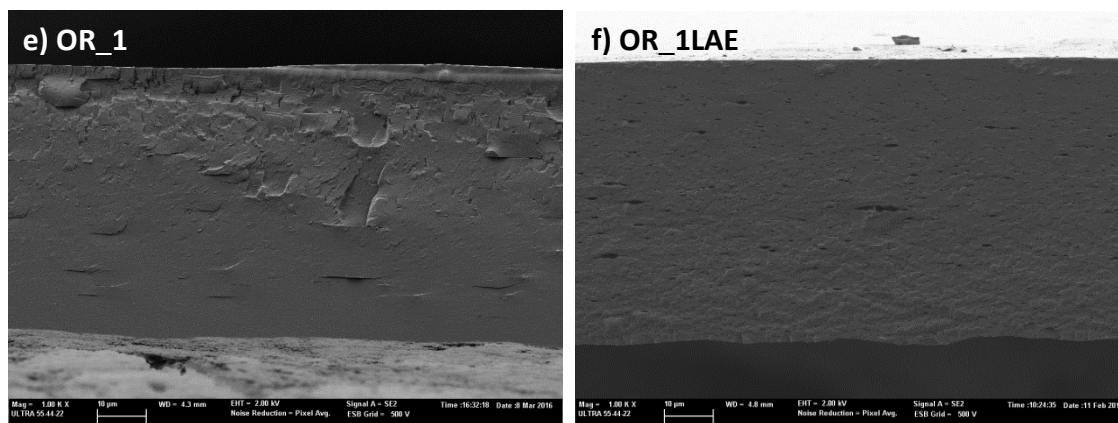
299 *FESEM analysis*

300 FESEM cross section images obtained for starch-gelatin blend films, with differing
301 degrees of oxidation, with and without LAE, are shown in Figure 1. In films with a non-
302 oxidised starch (OR_0), polymer separation can be observed during drying, the film
303 exhibiting a gelatin-rich layer at the top and a starch-rich layer at the bottom, depending
304 on their differing densities, as previously reported by Moreno et al. (2016). An oxidation
305 treatment of the starch seems to improve the polymer compatibility by enhancing
306 interactions between starch and gelatin chains; no clearly separated layers were
307 observed in the films with differing degrees of starch oxidation (OR_0.5 and OR_1),
308 showing a greater integration between both polymers. The enhanced cross linking ability
309 provided by OS also led to a smoother surface fracture in the cross section images of the
310 films, especially for the OR_1 sample, with the highest degree of oxidation.

311 The incorporation of LAE favoured the polymer compatibility in non-oxidised starch,
312 giving rise to a different film microstructure with small domains of both polymers due to
313 the LAE surfactant action (sample OR_0LAE); thus avoiding polymer stratification during
314 the film drying step, as reported by Moreno et al. (2016). With oxidized starch, films
315 containing LAE (OR_0.5LAE and OR_1LAE) showed a very smooth fracture surface,
316 thus indicating the good compatibility achieved by all the components. Only small voids
317 could be appreciated in the matrix, which can be attributed to the presence of very small
318 air bubbles incorporated during the homogenization step of the film-forming dispersion.

319 The surfactant effect of LAE promotes air incorporation and the high degree of viscosity
320 of the film-forming dispersion makes its elimination difficult. Microscopic observations
321 revealed a much more homogenous film structure when oxidised starch was used in the
322 starch-gelatin film formulation, which was clearly enhanced by LAE addition. In this case,
323 separate polymer domains were not observed and a cohesive structure without
324 discontinuities could be appreciated. This suggests LAE participation in the polymer
325 network, through its interaction/reaction with the new side groups of starch chains. The
326 LAE molecule has two primary amino groups that are highly reactive with the carbonyls
327 of oxidised starch and also two carbonyls which are potentially reactive with the amino
328 groups of protein. Therefore, the participation of LAE in polymer bonding could be
329 expected on the basis of its molecular structure.

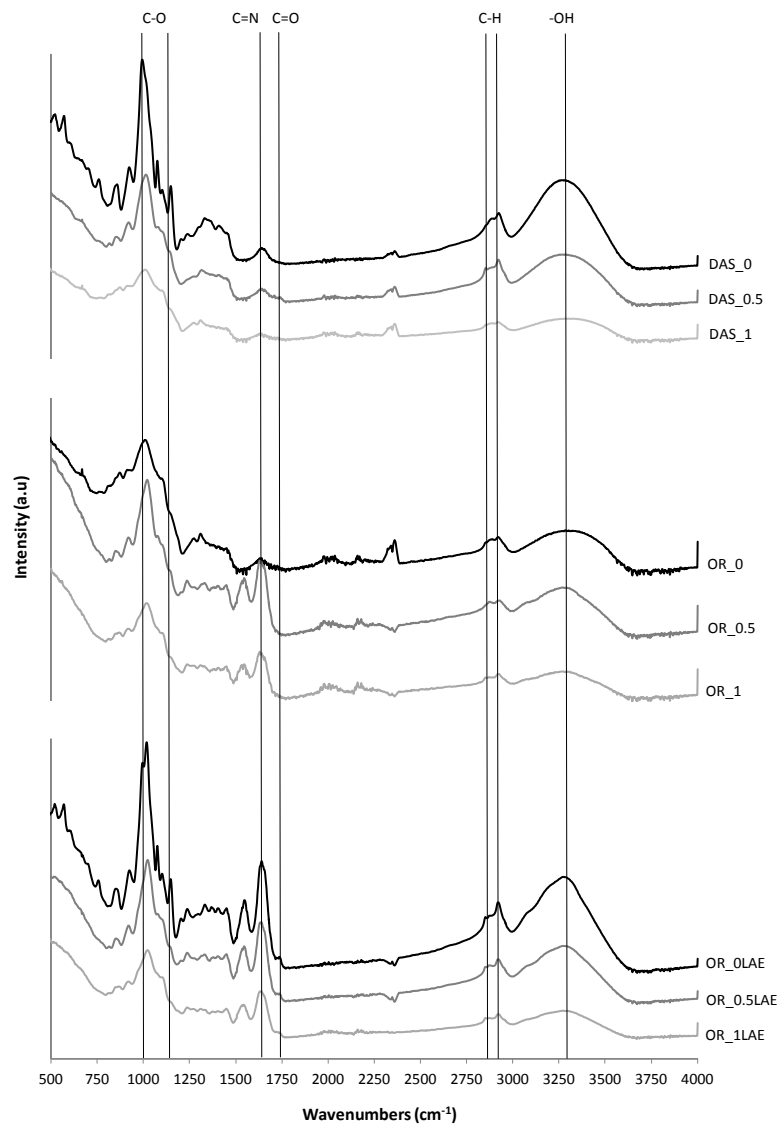




330 **Figure 1.** Micrographs obtained by FESEM of the cross-section of the films obtained
 331 from starch gelatin blends, with differing degrees of starch oxidation, and with or without
 332 LAE.

333 *ATR FTIR analysis*

334 Figure 2 shows the FTIR spectra of the different films, including pure starch films with
 335 differing degrees of oxidation. Non-oxidized starch-based films (DAS_0) showed
 336 characteristic peaks between 1000 and 1200 cm^{-1} , attributed to the C–O bond stretching
 337 of starch (Me et al., 2007; de Yu et al.); the peaks around 2850 and 2926 cm^{-1} , 1450 and
 338 1370 cm^{-1} are related to the C–H stretching and bending modes of the methylene (Sheng
 339 et al., 2011); the absorption around 1640 cm^{-1} is a typical band residing in the spectra of
 340 starch and its derivative, related to the tightly bound water (Seligra et al., 2016; Yu et al.,
 341 2010; Zhang et al., 2012), while the peak observed around 3300 cm^{-1} is associated with
 342 the stretching of OH groups from glucose, glycerol and water (Zhang et al., 2014). As
 343 the degree of oxidation increased, the absorbance of the bands associated with –OH
 344 groups exhibited a lower intensity, which could be related with the reduction of the –OH
 345 number in the starch chains and their lower water affinity. In fact, oxidation with periodate
 346 leads to the breakage of the C-2 and C-3 bonds of the anhydroglucose units, reducing
 347 the content of hydroxyl groups and forming aldehyde groups. Nevertheless, the
 348 characteristic absorption peak around 1740 cm^{-1} , corresponding to carbonyl (C=O)
 349 stretching vibration, presented a very weak intensity due to the formation of hemiacetal
 350 linkage between oxidised and non-oxidised starch residues (Zhang et al., 2007; Zhang
 351 et al., 2014). It is remarkable that the absorption peaks in samples with oxidised starch
 352 decreased in intensity at a constant wavenumber, as previously described by other
 353 authors (Rivero et al., 2010) for crosslinked polymer structures, probably associated with
 354 the major restrictions for bond vibration.



355

356 **Figure 2.** FTIR spectra of films obtained from starch films and starch gelatin blend
 357 films, with differing degrees of starch oxidation and with or without LAE.

358 Starch-gelatin blend films also exhibited a lower degree of intensity in the absorbance
 359 of the different bands, particularly those associated with the vibration of OH groups,
 360 which could be related with the strong interaction between both polymers forming a tight
 361 network where new bonds are formed. Particularly, dialdehyde polysaccharides are able
 362 to crosslink with amino groups of proteins through the formation of Schiff bases, imine
 363 group (C=N), which is associated with a stretching vibration around 1630 cm^{-1} (Azeredo
 364 and Waldron, 2016; Yin et al., 2008), as observed for both formulations with oxidised
 365 starch (OR_0.5, OR_1).

366 The incorporation of LAE introduced new C=O and NH_2 groups, with vibration bands
 367 at 1730 and 3400 cm^{-1} , respectively (Kamoun, 2015), which is reflected in a higher

368 relative intensity of these bands in samples containing this compound. Likewise, LAE
369 could also promote the formation of C=N groups, by reacting with both starch' carbonyls
370 or gelatin amino groups, as revealed by the relative intensity of the peak at 1630 cm⁻¹. A
371 higher intensity of the peaks, associated with the vibration of these groups, was noticed
372 when compared to the corresponding formulations without LAE; this could be related
373 with a greater ability of the network to permit bond vibration and to a greater
374 concentration of C=N groups. Thus, the carbonyl–amino reaction to form C=N groups
375 was enhanced by the presence of LAE. FTIR signal attenuation was also observed in
376 line with the degree of starch oxidation, which could be attributed to a more crosslinked
377 structure, as previously commented on.

378 From FTIR analyses, the crosslinking between starch and gelatin was evidenced, as
379 well as the participation of LAE in condensation reactions between amino groups and
380 carbonyls. Starch oxidation greatly promotes the inter-chain bonding between
381 polysaccharides and proteins, although the reaction probably involves, to a greater
382 extent, molecules of low molecular weight and higher molecular mobility and reactivity,
383 such as LAE, and short chain macromolecules resulting from the partial de-
384 polymerization of starch during oxidation, as described by Fiedorowicz and Para, (2006).
385 Edge-chain carbonyls of non-oxidised starch can also participate in the crosslinking
386 process. Likewise, cross-linked chains, by means of the formation of acetal bonds
387 between carbonyls and hydroxyls, can also contribute to the polymer network formed in
388 oxidised starch (Du et al., 2008), especially when no proteins were present (samples
389 DAS_0.5 and DAS_1.0).

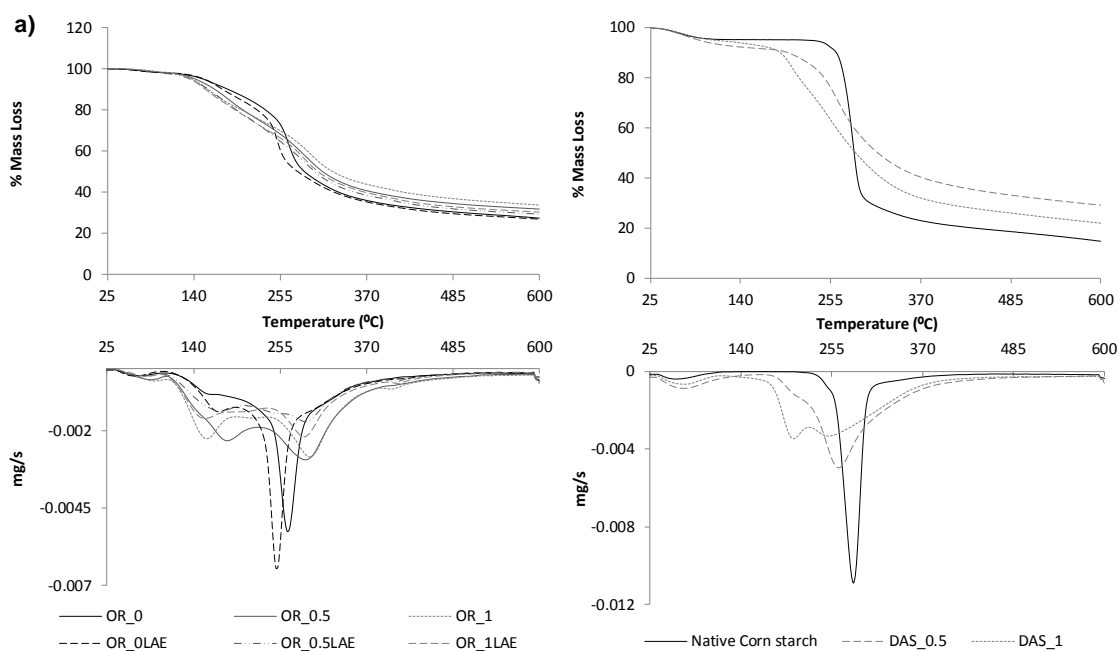
390

391 *Thermogravimetric analysis*

392 Figure 3 shows the thermograms obtained for the starch-gelatin films (a), with or
393 without LAE, and for pure starch (b), with differing degrees of oxidation. The evaluation
394 of the normalized mass loss curve with temperature for all of the formulations reflects a
395 slight initial loss, attributed to the water retained in the polymeric network, followed by a
396 pronounced mass loss associated with the polymer degradation. The oxidation of starch
397 greatly affected the thermo-stability of the polymer, decreasing the temperature of both
398 the onset and maximum degradation rates, as previously reported by other authors
399 (Soliman et al., 1997; Zhan et al., 2012), in line with a partial disruption of starch chains
400 (Fiedorowicz and Para, 2006). Likewise, two steps appeared in the thermo-degradation
401 process of oxidized starch, which were different for the two oxidized samples with

402 different molar ratio of SP. The first step can be attributed to the earlier degradation of
403 the more oxidized chains (more thermosensitive), which is more marked for sample
404 obtained with the highest ratio of oxidant, according to the greater progression of the
405 chain oxidations. The second step, extended to higher temperatures, can be attributed
406 to the thermal changes of crosslinked chains due to the formation of acetalic inter-chain
407 unions through the carbonyl side groups, as reported by Du et al., (2008). This
408 crosslinked structure in oxidized starch films was also deduced from FTIR spectra (as
409 commented on above) and its degradation at higher temperature can be expected
410 because of the higher molecular weight. Thus, an increase in the temperature range of
411 the overall degradation process occurred in oxidized starch samples. Therefore, the
412 different thermo-degradation behavior of starch treated with 0.5 and 1.0 molar ratio of
413 SP was coherent with the different oxidation level of both samples.

414 For starch-gelatin blend films, two main steps could be observed in polymer
415 degradation. The first one, which starts near 100 °C, must be attributed to the promotion
416 of the starch-protein reaction induced by the temperature increase. The rate of this step
417 was greatly increased by starch oxidation and LAE addition, on the basis of the
418 significantly lower ($p < 0.05$) onset temperature (T_0). This phenomenon points to the
419 prevailing reaction of the starch carbonyl groups with the protein amino groups, or to the
420 fact that LAE is bifunctional and reacts with both carbonyl or/and amino groups in this
421 first step. This behaviour indicates that starch-protein blend films cannot be obtained by
422 thermoplastic processing, especially if oxidized starch is used. The reaction of non-
423 oxidized starch and gelatin or LAE during the thermo-processing of blend films was
424 previously reported (Moreno et al. 2016), but this was greatly enhanced in OS due to the
425 extensive formation of carbonyl groups, which are highly reactive with protein amino
426 groups.



427

428 **Figure 3.** Thermogravimetric curves and the first derivatives of the TGA curves for
 429 film samples obtained from (a) starch-gelatin blends with differing degrees of starch
 430 oxidation, with or without LAE (b) starch with differing degrees of oxidation.

431 The second, and main, degradation step of the starch-gelatin films, characterized by
 432 the temperature of the fast degradation rate (T_{max}), reflected a significant increase
 433 ($p < 0.05$) in the T_{max} for films with OS, according to the previous formation of a crosslinked
 434 matrix during the first step. In this sense, it is remarkable that films containing LAE
 435 exhibited lower values of T_{max} , which suggests that the participation of LAE in the
 436 crosslinking reaction did not imply the formation of such a tight network, whereas a more
 437 continuous degradation/reaction process (less marked steps) was observed for films
 438 containing this compound and oxidized starch.

439 Thermal analysis reveals that starch-gelatin blend films are very sensitive, when the
 440 temperature rises above 100°C, which is greatly enhanced when the starch was
 441 oxidized, or other compounds containing amino or carbonyl groups, such as LAE, are
 442 present in the blend. These reactions promote uncontrolled crosslinking in the polymer
 443 network, which slowly degrades at higher temperatures. Therefore, the thermal
 444 processing of starch-gelatin blend films is limited by the occurrence of these uncontrolled
 445 reactions at high temperatures, also provoking the extensive formation of coloured
 446 compounds.

447 On the basis of the film's microstructure and crosslinking analysis, a high level of
 448 crosslinking between oxidised starch and gelatin chains can be expected in blend films,

449 especially when the highest ratio of oxidant was used. The addition of LAE implied its
450 participation in the bonding reactions, given that its molecule has carbonyl and amino
451 groups, which can compete with the macromolecules' functional groups, thus limiting the
452 inter-chain bonds. This occurred mainly when starch was less oxidised and there was
453 lower carbonyl concentration in its chains.

454

455 *3.2 Tensile, barrier and optical properties of the films*

456 *Tensile properties*

457 The values of the tensile parameters (elastic modulus (EM, MPa), tensile strength
458 (TS, MPa) and elongation at break (% E)), and the film thickness are shown in Table 1.
459 The differing degrees of starch oxidation clearly affected the tensile behaviour of the
460 films. The lower starch oxidation (OR_0.5 sample) led to a decrease in the stiffness while
461 increasing the stretchability of the films, in comparison with the non-oxidized formulation
462 (OR_0 sample). However, when the starch oxidation was higher (OR_1 sample), films
463 became more rigid and resistant, with lower extensibility. The crosslinking process
464 associated with starch oxidation involved an increase in the stiffness as a consequence
465 of the reinforcement of the matrix, but this trend was not observed for sample OR_0.5.
466 The poorer progress of chain bonding, together with the possible starch de-
467 polymerization during oxidation could yield a less cohesive polymeric network, thus
468 exhibiting lower strength in tensile behaviour.

469 The effect of LAE incorporation on tensile behaviour was dependent on the degree of
470 starch oxidation. When the oxidation was higher, LAE did not significantly affect the
471 tensile behaviour of the films. However, the extensibility of films with less oxidized starch
472 decreased when LAE was added, whereas it increased when LAE was added to non-
473 oxidized films. In both cases, LAE addition caused a decrease in stiffness and resistance
474 to break. These different effects, depending on the degree of oxidation of starch, could
475 be related with the different participation of this molecule in bonding reactions with
476 carbonyl groups of starch chains or amino groups of protein, as previously commented
477 on. At higher oxidation ratios, the carbonyls of the starch chains compete with those of
478 LAE with the highest concentration and their reaction with the protein chains could
479 promote inter-chain bonding. However, at lower oxidation ratios, there could be a greater
480 contribution of LAE reactions, which are less effective at promoting the network
481 cohesion, thus reducing the strength of the polymer matrix, but decreasing its
482 stretchability. In fact, due to its lower molecular weight, LAE would be more reactive with

483 carbonyl groups than gelatin and, consequently, it could be linked to the oxidized chains
 484 of starch, decreasing the degree of crosslinking of the polymer matrix. In the case of non-
 485 oxidised starch, the interfacial action of LAE between the polymer domains led to films
 486 with increased plastic deformability and lower strength, as reported by Moreno et al.
 487 (2016).

488

489 **Table 1.** Film thickness (μm) and moisture content; Tensile parameters (Elastic
 490 modulus (EM, MPa), Tensile Strength (TS, MPa) and deformation at break (% E)); Barrier
 491 properties (Water Vapor Permeability (WVP) and Oxygen Permeability (OP)); Colour
 492 coordinates (L^* , C_{ab}^* , h_{ab}^*) and internal transmittance (T_i) at 430 nm of the starch-gelatin
 493 blend films, with differing degrees of starch oxidation, with or without LAE, conditioned
 494 for 1 week at 53 % RH and 25 °C.

	OR_0		OR_0.5		OR_1	
	No LAE	LAE	No LAE	LAE	No LAE	LAE
Thickness (μm)	65 \pm 6 ^{b, y}	61 \pm 3 ^{a, x}	60 \pm 2 ^{a, x}	64 \pm 2 ^{b, y}	65 \pm 2 ^{b, x}	65 \pm 9 ^{b, x}
Xw (d.b. g water/ g dry film)	12,0 \pm 3,0 ^{b, x}	10,3 \pm 0,5 ^{b, x}	8,1 \pm 0,5 ^{a, x}	10,6 \pm 0,5 ^{b, y}	8,9 \pm 0,5 ^{a, y}	7,7 \pm 1,0 ^{a, x}
EM (MPa)	1020 \pm 190 ^{b, y}	510 \pm 90 ^{b, x}	470 \pm 70 ^{a, y}	360 \pm 70 ^{a, x}	1290 \pm 80 ^{c, x}	1300 \pm 200 ^{c, x}
TS (MPa)	33 \pm 6 ^{a, y}	24 \pm 7 ^{a, x}	21 \pm 6 ^{a, y}	35 \pm 6 ^{a, x}	46 \pm 8 ^{b, x}	46 \pm 8 ^{b, x}
% E	14 \pm 5 ^{b, x}	35 \pm 2 ^{c, y}	27 \pm 5 ^{c, y}	18 \pm 10 ^{b, x}	6,2 \pm 1,5 ^{a, x}	7 \pm 2 ^{a, x}
WVP x10⁷ (g·mm/kPa·h·m ²)	6,9 \pm 0,2 ^{c, y}	5,0 \pm 0,6 ^{a, x}	5,0 \pm 0,3 ^{b, x}	5,0 \pm 0,9 ^{a, x}	4,6 \pm 0,1 ^{a, x}	5,2 \pm 0,6 ^{a, y}
OP x10¹³ (cm ³ /m s Pa)	1,26 \pm 0,03 ^{b, x}	2,08 \pm 0,07 ^{b, y}	1,00 \pm 0,15 ^{ab, x}	2,50 \pm 0,50 ^{b, x}	0,75 \pm 0,09 ^{a, x}	0,95 \pm 0,11 ^{a, x}
L_{ab}[*]	80,6 \pm 0,5 ^{c, y}	73,8 \pm 0,6 ^{a, x}	76,8 \pm 1,1 ^{a, y}	73,4 \pm 1,0 ^{a, x}	78 \pm 0,8 ^{b, y}	73,8 \pm 0,4 ^{b, x}
C_{ab}[*]	7,27 \pm 0,17 ^{c, y}	4,41 \pm 0,08 ^{a, x}	28 \pm 2 ^{b, x}	28,3 \pm 0,7 ^{b, x}	33,3 \pm 1,0 ^{a, y}	29,2 \pm 0,7 ^{c, x}
h_{ab}[*]	98 \pm 0,3 ^{c, x}	104 \pm 0,9 ^{b, y}	81 \pm 2 ^{a, x}	79,2 \pm 0,5 ^{a, x}	91,2 \pm 0,7 ^{b, y}	79,1 \pm 0,6 ^{a, x}
T_i (430 nm)	0,833 \pm 0,004 ^{c, y}	0,826 \pm 0,005 ^{c, x}	0,74 \pm 0,02 ^{b, x}	0,73 \pm 0,014 ^{b, x}	0,689 \pm 0,016 ^{a, x}	0,711 \pm 0,004 ^{a, y}

495 *Different letters (a, b, c) in the same row indicate statistical differences ($p < 0.05$) between the*
 496 *formulations, either with or without LAE, with differing degrees of starch oxidation.*

497 *Different letters (x, y) in the same row indicate statistical differences ($p < 0.05$) between samples*
 498 *with and without LAE, for each degree of starch oxidation.*

499

500 The tensile behaviour of the films indicated that the degree of crosslinking of the
 501 starch-gelatin matrix, caused by the reaction between carbonyl and amino groups, did
 502 not progress to the same extent in the case of partial oxidation as a result of the
 503 heterogeneity of the chains (containing hydroxyl and carbonyl groups), which probably
 504 produces greater steric hindrances to the creation of new bonds. However, the

505 crosslinking effect for OR_1 films was much more noticeable, as reflected by the great
506 reinforcement of the polymer matrix. In the presence of LAE, the lower oxidation of starch
507 offers more opportunities for the reaction of LAE through its carbonyl groups, which did
508 not contribute to a reinforcement of the polymer matrix to the same extent as protein
509 linkages.

510

511 *Barrier properties*

512 Table 1 shows the values of the equilibrium moisture content of the films and their
513 barrier properties to water vapour and oxygen (WVP and OP). Starch oxidation led to a
514 significant ($p < 0.05$) decrease in the moisture content and WVP for both oxidation levels,
515 coherently with the greater hydrophobic nature of the matrix, resulting from the
516 transformation of $-OH$ into $-C=O$ groups in the starch chains (Zhang et al., 2007), and
517 the crosslinking effect, which created more resistance to mass transfer in the matrix. LAE
518 addition affected the moisture content of the films, reducing the value for non-oxidised
519 and most oxidised starch, but increasing the value at lower oxidation level. This also
520 points to differences in the network crosslinking when LAE is present, which affects the
521 active points for water adsorption, depending on the oxidation level. Oxygen permeability
522 was also significantly reduced ($p < 0.05$) by starch oxidation, which can also be related to
523 the tighter matrix caused by crosslinking and the milder water plasticising effect
524 associated with the lower water content. Only films containing LAE with a lower oxidation
525 level exhibited non-reduced oxygen permeability, which is coherent with the poorer
526 progress of the inter-chain bonds due to the LAE competence in the carbonyl-amino
527 reactions, previously commented on. Thus, starch oxidation allows less polar and tighter
528 polymer matrices to be obtained, with lower water affinity and enhanced barrier
529 properties, thus improving both water vapour and oxygen permeability. This is explained
530 by the weaker water plasticizing effect, since the films' moisture content falls, and also
531 by the crosslinking in the polymer network, which slows down the transport mechanisms
532 by promoting the tortuosity factor of the polymeric network.

533

534 *Optical properties*

535 Table 1 shows the values of the colour coordinates (L_{ab}^* , lightness; C_{ab}^* , chrome;
536 h_{ab}^* , hue) of the different films. Starch oxidation significantly reduced ($p < 0.05$) the
537 lightness and hue of films and gave rise to a significant ($p < 0.05$) increase in the chrome;

538 this is coherent with the formation of brown compounds resulting from the carbonyl-
539 amino reactions to form Maillard compounds, greatly promoted at the low moisture
540 content of the films. Specifically, the yellow-brown coloration associated with protein-
541 aldehyde reactions may be attributed to the formation of conjugated Schiff's bases, which
542 are intermediate products of the Maillard reaction (Cheftel et al., 1985; Martucci and
543 Ruseckaite,, 2009). In addition, when the LAE was incorporated, all of the oxidized
544 formulations exhibited a decrease in lightness and hue, obtaining browner films, which
545 is coherent with the involvement of LAE in the browning reactions, due to the presence
546 of amino and carbonyl groups in its molecular structure. Both the oxidized formulations
547 containing LAE and the film with lower degree of oxidation without LAE had very similar
548 colour coordinate values, whereas films with more oxidized starch without LAE were
549 slightly lighter and less red, thus indicating that browning progressed to a lesser extent
550 in this case, where a more effective polymer crosslinking was observed. On the other
551 hand, the incorporation of LAE into films with non-oxidised starch provoked a decrease
552 in the films' lightness and colour saturation, while also promoting the film yellowish, which
553 also points to the formation of coloured compounds to a certain extent.

554 The internal transmittance (T_i) of the films also decreased in line with starch oxidation,
555 mainly at lower wavelengths, where brown compounds absorb light Table 1 also shows
556 the values of T_i at 430 nm, which reflect that the higher the degree of starch oxidation,
557 the lower the T_i values. This behaviour was coherent with the selective absorption of
558 brown products (Maillard compounds) mainly coming from the reaction of low molecular
559 weight compounds, such as the reducing sugars resulting from the partial hydrolysis of
560 starch. Condensation reactions were encouraged by the greater availability of carbonyl
561 groups obtained during the oxidation process. The addition of LAE did not imply any
562 significant changes in the transmittance of the films, except for OD_1 films, for which its
563 addition led to an increase in internal transmittance. Crosslinking in the matrix can also
564 contribute to a reduction in internal transmittance due to the promotion of the film's
565 opacity (Martucci and Ruseckaite,, 2009).

566

567 *3.3. Water solubility, water uptake capacity and overall migration of the films.*

568 To analyse the effect that the crosslinking promoted by starch oxidation has on the
569 films' hydrophobicity, their water solubility, water uptake capacity and overall migration in
570 different food simulants were analysed.

571 Table 2 shows the water solubility values of the films, expressed as weight loss %

572 (WL %) in water, and the water uptake capacity (ΔW %) expressed as the mass of water
573 gained by the dry film. Starch oxidation led to a highly significant decrease ($p < 0.05$) in
574 the water uptake capacity of the films, coherently with the polarity reduction in the
575 polymeric matrix, in line with the fall in the number of $-OH$ groups, and by the
576 crosslinking of the polymer chains which restrict the water absorption by steric hindrance.
577 Nonetheless, the solubility in water (WL %) of the films was significantly greater ($p < 0.05$)
578 in the case of oxidized samples. The periodate oxidation of starch led to the formation of
579 dialdehyde starch, but also induced a disruption of the starch polysaccharide chains.
580 This fragmentation could result in both changes in the organization of starch chains and
581 solubility (Fiedorowicz and Para, 2006).

582 On the other hand, the addition of LAE involved a significant increase ($p < 0.05$) in
583 solubility, while significantly reducing the water uptake values for both oxidized
584 formulations, contrary to what occurred for non-oxidized films. The higher solubility
585 values of oxidized films with LAE could be explained by its tighter attachment to the
586 carbonyl groups present in the low molecular weight molecules resulting from the partial
587 hydrolysis of starch, which were easily released into the water. Likewise, the reduction
588 in the water uptake capacity produced by LAE is coherent with the involvement of this
589 molecule in the crosslinking of the polymers, thus cooperating in the steric limitation of
590 water absorption in the network.

591 Table 2 summarizes the mean values of the overall migration of the films into food
592 stimulants with differing polarity: simulant A (ethanol 10% v/v, simulating food of
593 hydrophilic nature), simulant B (acetic acid 3% w/v, simulating food of hydrophilic nature
594 and pH below 4.5) and simulant D2 (isooctane, simulating food of lipophilic nature and
595 with free surface fats). All of the film formulations exceeded the threshold level of 10
596 mg/dm^2 established by the current law (Commission Regulation (EU) No 10/2011) for
597 every simulant, the highest values being obtained in the acid medium. However, the
598 oxidized formulation in 3 % acetic acid had significantly ($p < 0.05$) lower migration values
599 than non-oxidized formulations. This suggests that crosslinking was effective at reducing
600 the disintegration action of the acid medium, thus limiting the release of film compounds.
601 On the contrary, the oxidized films showed a significantly ($p < 0.05$) higher degree of
602 migration in ethanol 10 % (v/v) than the non-oxidised. This could be attributed to the
603 formation of low molecular compounds during the oxidation process, which is more easily
604 released into the aqueous media. No significant differences were noticed for the different
605 films' migration in isooctane. The addition of LAE only affected the migration values in
606 the films with non-oxidised starch, promoting their release in aqueous media at neutral

607 and acid pH. This agrees with the partial attachment of LAE to the polymer network in
 608 oxidised matrices, as previously commented on, thus restricting its migration observed
 609 in non-oxidised matrices.

610

611 **Table 2.** Overall migration values (mg dm⁻²) of the different films into different food
 612 simulants (A: ethanol (10% v/v), B: acetic acid (3% w/v), D2: isooctane) and weight loss
 613 (WL%, g per100 g dried film) and water uptake ($\Delta W\%$, g water per 100 g dried film) of
 614 the films after 24 h of immersion in distilled water at 25 °C. Mean values and standard
 615 deviation.

	Overall migration values			WL %	$\Delta W\%$
	Etanol 10% (v/v)	Acetic Acid 3% (w/v)	Isooctane		
OR_0	108 ±15 ^{a, y}	362 ±36 ^{a, z}	47 ±24 ^{a, x}	35 ±3 ^{m, 1}	1544 ±25 ^{n, 1}
OR_0LAE	348 ±52 ^{c, y}	622 ±148 ^{b, z}	126 ±99 ^{a, x}	37 ±4 ^{m, 1}	2015 ±40 ^{n, 2}
OR_0.5	243 ±30 ^{b, y}	236 ±21 ^{a, y}	51 ±65 ^{a, x}	40.4 ±0.4 ^{n, 1}	374 ±115 ^{m, 2}
OR_0.5LAE	260 ±18 ^{b, y}	277 ±16 ^{a, y}	29 ±5 ^{a, x}	46.6 ±0.8 ^{n, 2}	182 ±28 ^{m, 1}
OR_1	218 ±40 ^{b, y}	247 ±20 ^{a, y}	25 ±32 ^{a, x}	40.1 ±0.3 ^{n, 1}	367 ±78 ^{m, 2}
OR_1LAE	237 ±3 ^{b, y}	280 ±8 ^{a, z}	30,1 ±0,5 ^{a, x}	46.7 ±0.7 ^{n, 2}	133 ±20 ^{m, 1}

616 *Different letters in the same column indicate statistical differences ($p < 0.05$) between the*
 617 *formulations for the same simulant (a, b, c) or between samples with the differing degree of starch*
 618 *oxidation (m, n).*

619 *Different letters (x, y, z) in the same column indicate statistical differences ($p < 0.05$) between*
 620 *simulants for each formulation.*

621 *Different numbers (1, 2) in the same column indicate significant differences ($p < 0.05$) between*
 622 *samples, with and without LAE*

623

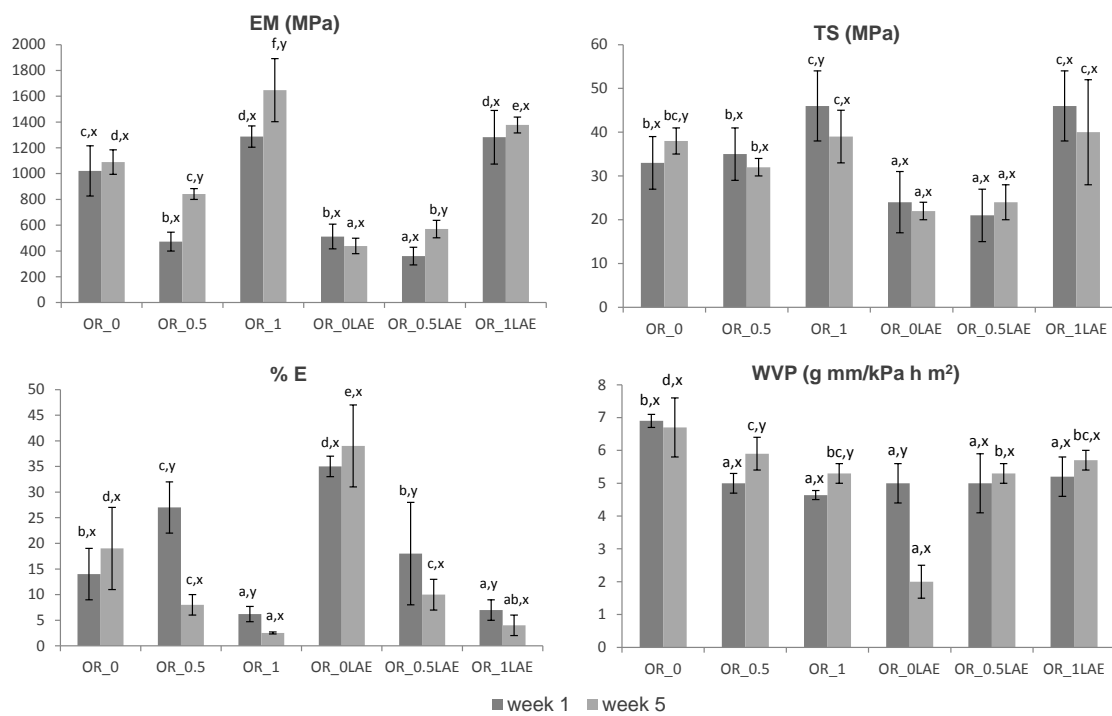
624 Starch oxidation and the subsequent crosslinking to gelatin greatly limit the water
 625 uptake capacity of the films, although they did not reduce either the film's water solubility
 626 or the migration values into neutral aqueous food simulants. Nevertheless, crosslinked
 627 films were more resistant to the acid systems, coherent with the formation of a tight
 628 network. The partial disruption of starch chains by oxidation led to an increase in the
 629 soluble fraction of the films. In the same sense, the addition of a low molecular weight
 630 compound (LAE) promoted the film's solubility in water and its migration into aqueous
 631 food simulants.

632

633 **3.4 Effect of starch oxidation on the stability of the film properties.**

634 For the purposes of evaluating the potential progress of both Maillard and crosslinking
 635 reactions in the film network throughout time, the colour parameters, tensile properties
 636 and water vapour barrier capacity of the films were analysed after 5 storage weeks at
 637 53 % RH and 25 °C.

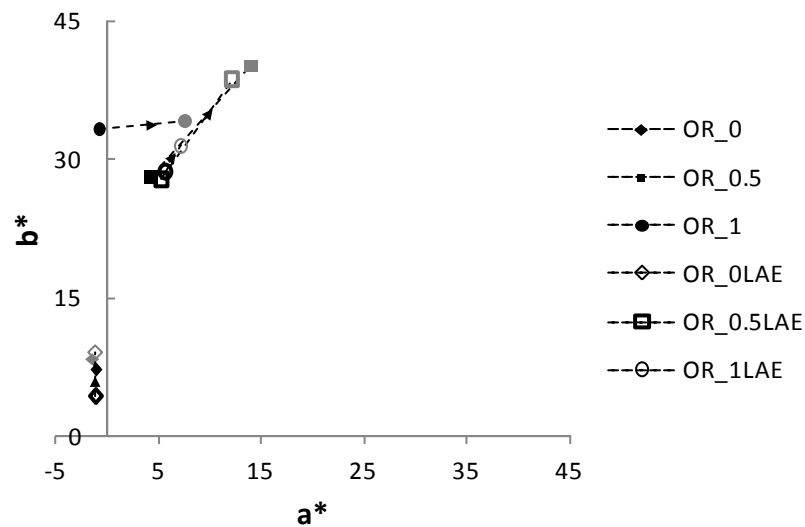
638 Figure 4 compares the values of the tensile properties of the films (EM, TS and % E)
 639 and WVP obtained after 1 and 5 weeks of storage. The results obtained pointed to a
 640 progression of the crosslinking process throughout storage time in oxidised formulations,
 641 since the two films with oxidised starch, both the one with and the one without LAE,
 642 exhibited a remarkable increase ($p < 0.05$) in EM and a decrease in the film extensibility.
 643 Likewise, a slight increase in WVP was observed for these samples when there was no
 644 LAE in the formulation.



645
 646 **Figure 4.** Effect of storage time (1 and 5 weeks) on the tensile parameters (EM, TS
 647 and % E) and Water Vapour Permeability (WVP) of the starch-gelatin blend films, with
 648 differing degrees of starch oxidation, with or without LAE films, conditioned at 53 % RH.
 649 Mean values and standard deviation. Different letters (a, b, c, d, e, f) indicate significant
 650 differences ($p < 0.05$) between the different film formulations for the same conditioning
 651 time. Different letters (x, y) indicate significant differences ($p < 0.05$) between both
 652 conditioning times for the same formulation.

653
 654 On the other hand, the colour of the films also changed during storage. Figure 5 shows

655 the *locust* of the different films in the a*b*chromatic diagram after 1 and 5 weeks of
 656 storage; here, although no notable changes can be appreciated for the films with non-
 657 oxidised starch, either with or without LAE, those films containing oxidized starch evolved
 658 towards a redder hue with higher colour saturation. These chromatic changes were
 659 associated with a 16% reduction in lightness for the films with lower starch oxidation,
 660 both with and without LAE, a 9 % reduction for the LAE-free sample with the most
 661 oxidised starch and a 10% increase in the case of non-oxidized starch with LAE. These
 662 colour changes also indicate the progression of the formation of conjugated Schiff's
 663 bases (intermediate products of the Maillard reaction) causing an increase in colour
 664 intensity (Martucci and Ruseckaite, 2009) throughout storage. Browning reactions
 665 progressed to a greater extent in the films with oxidized starch, thus indicating the
 666 progressive reaction between carbonyls and amino groups. The films with lower
 667 oxidation level exhibited the greatest changes, both with and without LAE, whereas in
 668 the case of those with the highest oxidation ratio, the browning of the films with LAE was
 669 more limited. However, the colour of the LAE-free films with the highest oxidation degree,
 670 which exhibited less initial browning, changed until they reached similar browning levels
 671 to the OR_1LAE sample.



672

673 **Figure 5.** Colour development in the a*b* chromatic diagram of the starch-gelatin films
 674 conditioned at 53 % RH and 25°C. (1 week: black marks, and 5 weeks: grey marks)

675

676

677 The browning reactions progressed in oxidized starch films, mainly in those with lower

678 oxidation degree, giving rise to more coloured films, which can limit their application.
679 Nevertheless, these Maillard compounds have antimicrobial activity (Hauser et al., 2014;
680 Wu et al., 2014), which could improve the films' functionality, imparting active properties.

681

682 3.5 Antimicrobial activity of the films

683 Table 3 summarizes the results of the *in vitro* antimicrobial test carried out for the
684 different films, with and without LAE. The bacterial counts after 24 h of incubation, as
685 well as the growth inhibition with respect to the inoculum control of each bacteria are
686 shown. A total growth inhibition was observed for all films containing LAE, thus indicating
687 the high antimicrobial effectiveness of this compound released from the films. Likewise,
688 LAE-free films with oxidized starch also significantly ($p < 0.05$) inhibited the growth of both
689 bacteria, although to a lesser extent than the films containing LAE. This mild antimicrobial
690 activity can be attributed to the formed brown compounds (Maillard reaction) and their
691 release from the films. The antimicrobial activity of Maillard compounds has been
692 associated with the generation of hydrogen peroxide (Hauser et al., 2014). OS:BG_1
693 films (with highest starch oxidation degree) provoked the highest ($p < 0.05$) growth
694 inhibition of both bacteria, in agreement with the higher production of Maillard
695 compounds, as deduced from colour parameters (Table 1). The Gram positive bacterium
696 (*L. innocua*) was significantly more ($p < 0.05$) sensitive to the antimicrobial action of brown
697 compounds present in the films.

698

699

700

701

702

703

704

705 **Table 3.** Effect of the films on the growth and survival of *Listeria innocua* (CECT 910)
706 and *Escherichia coli* (CECT 101) after 24 h at 37 °C. Average values and standard
707 deviation.

	Bacterial growth (log CFU/mL)		Growth inhibition (log CFU/mL)	
	<i>E.coli</i>	<i>L.innocua</i>	<i>E.coli</i>	<i>L.innocua</i>
Control	8.9 ±0.08 ^{c, 1}	9.21 ±0.05 ^{c, 2}	-	-
OS:BG_0	9.13 ±0.06 ^{d, 1}	9.15 ±0.14 ^{c, 1}	-0.21 ±0.06 ^{a, 1}	0.05 ±0.14 ^{a, 2}
OS:BG_0LAE	NCD*	NCD*	TOTAL	TOTAL
OS:BG_0.5	8.34 ±0.14 ^{b, 1}	8.0 ±0.5 ^{b, 1}	0.58 ±0.14 ^{b, 1}	1.2 ±0.5 ^{b, 2}
OS:BG_0.5LAE	NCD*	NCD*	TOTAL	TOTAL
OS:BG_1	8.07 ±0.013 ^{a, 2}	7.36 ±0.08 ^{a, 1}	0.841 ±0.013 ^{c, 1}	1.85 ±0.08 ^{b, 2}
OS:BG_1LAE	NCD*	NCD*	TOTAL	TOTAL

708 *No Cells Detected

709 Different letters (a, b) in the same column indicate statistical differences ($p < 0.05$) between
710 formulations for each bacterium.

711 Different numbers (1, 2) in the same row indicate statistical differences ($p < 0.05$) between
712 bacteria for each formulation.

713

714 Conclusion

715 Starch oxidation with sodium periodate greatly promoted crosslinking in starch-gelatin
716 (1:1) films, enhancing the films' strength and oxygen and water vapour barrier capacity,
717 while reducing their water uptake capacity and migration to acid media. A
718 glucose:periodate molar ratio of 1:1 was more effective than 1:0.5, due to the greater
719 progress of di-aldehyde formation, which offers more reactive groups for the amino-
720 carbonyl reaction and the formation of inter-chain bonds between polysaccharides and
721 proteins. Incorporating LAE as an antimicrobial compound interferes with the polymer
722 crosslinking reactions due to its bifunctional nature (it contains carbonyl and amino
723 groups which also react with the polymer chains), especially when there was a lower
724 degree of starch oxidation because of the lower ratio of oxidant. This affected the tensile
725 behaviour of the films, which were less stiff and stretchable. Nevertheless, an amino-
726 carbonyl condensation reaction also provoked browning in the films, in line with the
727 formation of Maillard compounds. This browning, as well as crosslinking, progressed in
728 the film network throughout storage, especially in the less oxidized starch films, which
729 could compromise their application for certain uses. The formation of Maillard
730 compounds conferred antibacterial activity to the films, while the incorporation of LAE
731 produced a total bactericidal effect. Based on the lower browning progression, reduced
732 water sensitivity, better mechanical performance and the higher antimicrobial activity,
733 blend films with the most oxidized starch and gelatin containing LAE are promising
734 materials for food packaging applications. In order to further improve the film
735 performance, future studies should address film application on real food systems, aiming
736 to quantify the real effect of both Maillard compounds and LAE on the product microbial
737 quality and shelf life.

738 **Acknowledgements**

739 The authors acknowledge the financial support provided by Ministerio de Economía
740 y Competitividad (Projects AGL2013-42989-R and AGL2016-76699-R). The authors
741 also thank Oscar Gil and Amparo Ribes from the Institute of Materials Technology (UPV)
742 for the support and assistance in the use of the infrared spectrometer and the services
743 rendered by the Electron Microscopy Service of the UPV. Olga Moreno Marro also
744 thanks the Ministerio de Educación, Cultura y Deporte for the FPU 2012-1121 grant.

745 **REFERENCES**

- 746 Acosta, S., Jiménez, A., Cháfer, M., González-Martínez, C., & Chiralt, A. (2015). Physical
747 properties and stability of starch-gelatin based films as affected by the addition of esters of
748 fatty acids. *Food Hydrocolloids*, 49, 135-143.
- 749 ASTM. (1995). Standard test methods for water vapour transmission of materials. In Standard
750 designations: E96-95 annual book of ASTM standards. Philadelphia, PA: American Society
751 for Testing and Materials.
- 752 ASTM. (2001). Standard test method for tensile properties of thin plastic sheeting. In Standard
753 D882 annual book of American Standard Testing Methods. Philadelphia, PA: American
754 Society for Testing and Materials. ASTM.
- 755 ASTM. (2005). Standard test method for oxygen gas transmission rate through plasticfilm and
756 sheeting using a coulometric sensor. In Standard designation: D3985-05:annual book of
757 American Society for Testing Materials. West Conshohocken, PA: ASTM.
- 758 Atarés, L., Bonilla, J., & Chiralt, A. (2010). Characterization of sodium caseinate-based edible
759 films incorporated with cinnamon or ginger essential oils. *Journal of Food Engineering*, 100(4),
760 678-687.
- 761 Azeredo, H. M., & Waldron, K. W. (2016). Crosslinking in polysaccharide and protein films and
762 coatings for food contact—A review. *Trends in Food Science & Technology*, 52, 109-122. Bakal,
763 G., & Diaz, A. (2005). The lowdown on lauric arginate. *Food Quality*, 12(1), 54-61.
- 764 Balaguer, M. P., Gómez-Estaca, J., Gavara, R., & Hernandez-Munoz, P. (2011). Biochemical
765 properties of bioplastics made from wheat gliadins cross-linked with cinnamaldehyde. *Journal*
766 *of agricultural and food chemistry*, 59(24), 13212-13220.
- 767 Barnett, I., (2011). Packaging Solutions Throughout the Supply Chain: Technology, Trends and
768 Future Outlook. *Business Insight*, London.
- 769 Byun, Y., & Kim, Y. T. (2014). Chapter 14 – Bioplastics for food packaging: Chemistry and
770 physics. In J. H. Han (Ed.), *Innovations in food packaging* (2nd ed., pp. 353–368). San Diego:
771 Academic Press.
- 772 Cazón, P., Velazquez, G., Ramírez, J. A., & Vázquez, M. (2016). Polysaccharide-based films and
773 coatings for food packaging: A review. *Food Hydrocolloids*.
- 774 Cheftel, J.C., Cuq, J.-L., Lorient, D., 1985. Amino acids, peptides, and proteins. In: Fennema,
775 O.R. (Ed.), *Food Chemistry*. Marcel Dekker, New York, pp. 245–369.
- 776 Commission Regulation (EU) No. 10/2011 of 14 January 2011 on plastic materials and articles
777 intended to come into contact with food.

- 778 Du, Y. L., Cao, Y., Lu, F., Li, F., Cao, Y., Wang, X. L., & Wang, Y. Z. (2008). Biodegradation
779 behaviors of thermoplastic starch (TPS) and thermoplastic dialdehyde starch (TPDAS) under
780 controlled composting conditions. *Polymer Testing*, 27(8), 924-930.
- 781 Fakhoury, F. M., Martelli, S. M., Bertan, L. C., Yamashita, F., Mei, L. H. I., & Queiroz, F. P. C.
782 (2012). Edible films made from blends of manioc starch and gelatin—Influence of different types
783 of plasticizer and different levels of macromolecules on their properties. *LWT-Food Science
784 and Technology*, 49(1), 149-154.
- 785 Fiedorowicz, M., & Para, A. (2006). Structural and molecular properties of dialdehyde starch.
786 *Carbohydrate Polymers*, 63(3), 360-366.
- 787 Hauser C., Müller U., Sauer T., Augner K., Pischetsrieder. (2014). Maillard reaction products as
788 antimicrobial components for packaging films. *Food chemistry*, 145, 603-613.
- 789 Hawkins, D.R., Rocabayera, X., Ruckman, S., Segret, R., Shaw, D. (2009). Metabolism and
790 pharmacokinetics of ethyl Na-lauroyl-L-arginate hydrochloride in human volunteers. *Food and
791 Chemical Toxicology*, 47, 2711–2715.
- 792 Higuera, L., López-Carballo, G., Hernández-Muñoz, P., Gavara, R., & Rollini, M. (2013).
793 Development of a novel antimicrobial film based on chitosan with LAE (ethyl-N α -dodecanoyl-
794 L-arginate) and its application to fresh chicken. *International journal of food microbiology*,
795 165(3), 339-345.
- 796 Hutchings, J. B. (1999). *Food and colour appearance* (2nd ed.). Gaithersburg, MD: Chapman and
797 Hall/Food Science Book/Aspen Publication.
- 798 Jiménez, A., Fabra, M. J., Talens, P., & Chiralt, A. (2012). Edible and biodegradable starch films:
799 a review. *Food and Bioprocess Technology*, 5(6), 2058-2076.
- 800 Kamoun, E. A. (2016). N-succinyl chitosan–dialdehyde starch hybrid hydrogels for biomedical
801 applications. *Journal of advanced research*, 7(1), 69-77.
- 802 Martucci, J. F., & Ruseckaite, R. A. (2009). Tensile properties, barrier properties, and
803 biodegradation in soil of compression—Molded gelatin-dialdehyde starch films. *Journal of
804 Applied Polymer Science*, 112(4), 2166-2178.
- 805 McHugh, T. H., Avena-Bustillos, R., & Krochta, J. M. (1993). Hydrophobic edible films: modified
806 procedure for water vapor permeability and explanation of thickness effects. *Journal of Food
807 Science*, 58(4), 899–903.
- 808 Moreno, O., Pastor, C., Muller, J., Atarés, L., González, C., & Chiralt, A. (2014). Physical and
809 bioactive properties of corn starch–Buttermilk edible films. *Journal of Food Engineering*, 141,
810 27-36.
- 811 Moreno, O., Atarés, L., & Chiralt, A. (2015). Effect of the incorporation of antimicrobial / antioxidant
812 proteins on the properties of potato starch films. *Carbohydrate polymers*, 133, 353-364.
- 813 Moreno, O., Díaz, R., Atarés, L., & Chiralt, A. (2016). Influence of the processing method and
814 antimicrobial agents on properties of starch-gelatin biodegradable films. *Polymer International*,
815 65, 904-914
- 816 Muriel-Galet, V., López-Carballo, G., Hernández-Muñoz, P., & Gavara, R. (2014).
817 Characterization of ethylene-vinyl alcohol copolymer containing lauril arginate (LAE) as
818 material for active antimicrobial food packaging. *Food packaging and shelf life*, 1(1), 10-18.

- 819 Ortega-Toro, R., Jiménez, A., Talens, P., & Chiralt, A. (2014). Properties of starch–hydroxypropyl
820 methylcellulose based films obtained by compression molding. *Carbohydrate polymers*, 109,
821 155-165.
- 822 Rhim, J. W., Gennadios, A., Weller, C. L., Cezeirat, C., & Hanna, M. A. (1998). Soy protein
823 isolate–dialdehyde starch films. *Industrial Crops and Products*, 8(3), 195-203.
- 824 Rivero, S., García, M. A., & Pinotti, A. (2010). Crosslinking capacity of tannic acid in plasticized
825 chitosan films. *Carbohydrate Polymers*, 82(2), 270-276.
- 826 Rodríguez, E., Seguer, J., Rocabayera, X., Manresa., A. (2004) Cellular effects of
827 monohydrochloride of L-arginine, Na-lauroyl ethylester (LAE) on exposure to Salmonella
828 typhimurium and Staphylococcus aureus. *Journal of Applied Microbiology*. 96, 903–912.
- 829 Seligra, P. G., Jaramillo, C. M., Famá, L., & Goyanes, S. (2016). Biodegradable and non-
830 retrogradable eco-films based on starch–glycerol with citric acid as crosslinking agent.
831 *Carbohydrate polymers*, 138, 66-74.
- 832 Sheng, Y., Wang, Q. H., Xu, X. C., Jiang, W. Y., Gan, S. C., & Zou, H. F. (2011). Oxidation of
833 cornstarch using oxygen as oxidant without catalyst. *LWT - Food Science and Technology*,
834 44, 139–144.
- 835 Soliman, A. A., El-Shinnawy, N. A., & Mobarak, F. (1997). Thermal behaviour of starch and
836 oxidized starch. *Thermochimica Acta*, 296(1), 149-153.
- 837 Tharanathan, R. N. (2003). Biodegradable films and composite coatings: past, present and future.
838 *Trends in Food Science & Technology*, 14(3), 71-78.
- 839 Wang, X., Gu, Z., Qin, H., Li, L., Yang, X., & Yu, X. (2015). Crosslinking effect of dialdehyde
840 starch (DAS) on decellularized porcine aortas for tissue engineering. *International Journal of*
841 *Biological Macromolecules*, 79, 813-821.
- 842 Wu Shuping., Hu Jiao., Wei Liuting., Du Y., Shi X., Zhang L. (2014). Antioxidant and antimicrobial
843 activity of Maillard reaction products from xylan with chitosan/chitooligomer/ glucosamine
844 hydrochloride/taurine model systems. *Food Chemistry* 143, 148-203
- 845 Yin, Q. F., Ju, B. Z., Zhang, S. F., Wang, X. B., & Yang, J. Z. (2008). Preparation and
846 characteristics of novel dialdehyde aminothiazole starch and its adsorption properties for Cu
847 (II) ions from aqueous solution. *Carbohydrate Polymers*, 72(2), 326-333.
- 848 Yu, J., Chang, P. R., & Ma, X. (2010). The preparation and properties of dialdehyde starch and
849 thermoplastic dialdehyde starch. *Carbohydrate Polymers*, 79(2), 296-300.
- 850 Zhang, L., Zhang, S., Dong, F., Cai, W., Shan, J., Zhang, X., & Man, S. (2014). Antioxidant activity
851 and in vitro digestibility of dialdehyde starches as influenced by their physical and structural
852 properties. *Food chemistry*, 149, 296-301.
- 853 Zhang, S. D., Zhang, Y. R., Zhu, J., Wang, X. L., Yang, K. K., & Wang, Y. Z. (2007). Modified
854 corn starches with improved comprehensive properties for preparing thermoplastics. *Starch-*
855 *Stärke*, 59(6), 258-268.
- 856 Zhang, Y. R., Wang, X. L., Zhao, G. M., & Wang, Y. Z. (2012). Preparation and properties of
857 oxidized starch with high degree of oxidation. *Carbohydrate Polymers*, 87(4), 2554-2562.
- 858